JPE 16-1-4

http://dx.doi.org/10.6113/JPE.2016.16.1.27
ISSN(Print): 1598-2092 / ISSN(Online): 2093-4718

A Mixed SOC Estimation Algorithm with High Accuracy in Various Driving Patterns of EVs

Dong-Jin Lim*, Jung-Hoon Ahn*, Dong-Hee Kim*, and Byoung Kuk Lee†

*,†Department of Electrical and Computer Engineering, Sungkyunkwan University, Suwon, Korea

Abstract

In this paper, a mixed algorithm is proposed to overcome the limitations of the conventional algorithms, which cannot be applied in various driving patterns of drivers. The proposed algorithm based on the coulomb counting method is mixed with reset algorithms that consist of the enhanced OCV reset method and the DCIR iterative calculation method. It has many advantages, such as a simple model structure, low computational overload in various profiles, and a low accumulated SOC error through the frequent SOC reset. In addition, the enhanced parameter based on a mathematical analysis of the second-order RC ladder model is calculated and is then applied to all of the methods. The proposed algorithm is verified by experimental results based on a 27-Ah LiPB. It is observed that the SOC RMSE of the proposed algorithm decreases by about 9.16% compared to the coulomb counting method.

Key words: Coulomb counting method, DCIR reset method, Enhanced OCV reset method, Mixed algorithm, SOC estimation algorithm, Various driving patterns

I. INTRODUCTION

A battery management system (BMS) is considered to be a key technology for safe and efficient operation of electric vehicles (EVs) [1]-[3]. Among the various factors managed by a BMS, the state of charge (SOC) is the most important because it is used as an indicator to protect the battery against over-charge and over-discharge. Moreover, through an accurate estimation of the SOC, the usable range of the battery can be extended, i.e., EVs can be driven longer.

A coulomb counting method (CCM) is generally used to estimate the SOC because of its ease of implementation and robustness to noise [4]-[6]. The CCM estimates the SOC by accumulating charges based on the initial value of a battery charge. However, the CCM has an error due to the current measurements made by current sensors to sense current through physical sensors. Even though the current sensor of a BMS has a high accuracy, it also has a small error. In case of the CCM, the battery current is continuously accumulated, which further results in an inevitable accumulation of a small error into a large error. As the time advances, this problem of an accumulated error of the battery current in the CCM is aggravated.

Therefore, various algorithms have been recently developed to solve the problem of an accumulated error in the CCM. Among the various algorithms, the extended Kalman filter (EKF) [7]-[12] is an intelligent mathematical tool for estimating the present state of a non-linear dynamic system. Because the battery has non-linear properties, the EKF is an effective solution for SOC estimation. Meanwhile, neural networks (NNs) [13]-[15] are a family of statistical learning models inspired by biological neural networks. They can solve complex, uncertain, and non-linear problems like SOC estimation. Since the EKF and NNs only use the present values of the current and voltage without accumulated operations of the battery current when compared to the CCM, these algorithms do not generate the accumulated error. In the SOC reset method [16], [17], the accumulated SOC error occurring in the CCM can be actively reduced by resetting the initial SOC of a battery. This means that the accumulated current error is also initialized to zero.

Previously described algorithms have only been verified for a specific profile. However, in EVs, such verification cannot insure estimation accuracy because the actual current profiles of the batteries for EVs are very diverse depend on the driver's driving pattern. For example, in the case of highway driving at

Manuscript received Sep. 17, 2015; accepted Dec. 9, 2015
Recommended for publication by Associate Editor Jonghoon Kim.
†Corresponding Author: bkleeskku@skku.edu
Tel: +82-31-299-4581, Fax: +82-31-299-4612, Sungkyunkwan University
*Dept. of Electrical & Computer Eng., Sungkyunkwan University, Korea

a constant speed, the current profile may be monotonous. However, if a vehicle is operated at various speeds with frequent stop as in urban driving, its current profile is more dynamic. Thus, without considering the various current profiles of EVs, a highly reliable and accurate SOC estimation algorithm cannot be achieved. In other words, the SOC algorithm for an EV needs to achieve high reliability for all current profiles.

However, the above-mentioned algorithms [7]-[17] are insufficient to meet this requirement. Especially, the mathematical approaches such as EKF and NNs have to be exponentially complex to cover various profiles. This complexity cause a computational overload of the arithmetic unit which has a physical limitation. Meanwhile, in the case of SOC reset algorithms, which are only effective in specific current conditions, the reliability of their estimation performance can be seriously decreased in other profiles where they do not meet any reset conditions. In summary, the conventional SOC estimation algorithms cannot provide a high reliability in terms of their performance for the various profiles.

In this paper, a mixed SOC reset algorithm, which has a low computational burden and high reliability in various current profiles, is proposed. The large coverage of the SOC reset is the most important factor for selecting the algorithm pair to be mixed. Thus, two representative algorithms, which operate independently in the driving or stop sections, are selected in order to cover various driving patterns. Moreover, to maximize the estimation performance, the key parameter for the reset is rationally redefined based on a detail analysis of each algorithm. As a result, the proposed algorithm is able to perform the SOC reset even at a low computational load and for various profiles. The proposed algorithm is verified with the help of experimental results by using a Kokam 27-Ah LiPB in four driving patterns, which consist of the urban dynamometer-driving schedule (UDDS) profile and the highway fuel economy test (HWFET) profile.

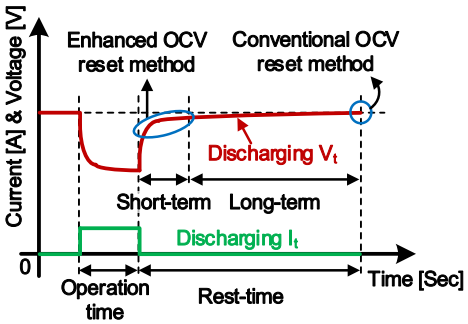

(a) Region of enhanced OCV reset in discharge.

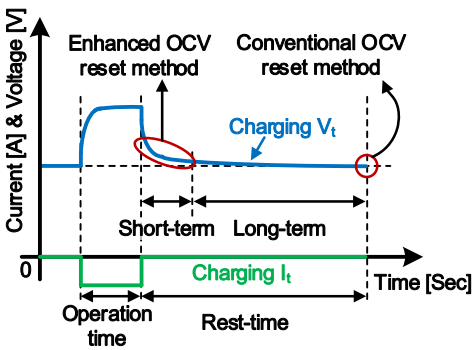

(b) Region of enhanced OCV reset in charge.

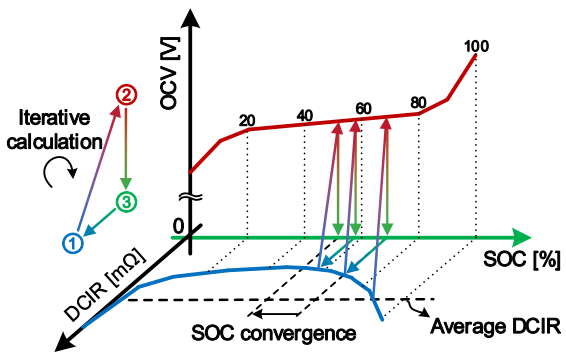

(c) Principle of algorithm using the DCIR iterative calculation.

Fig. 1. Operation principle of the SOC reset algorithms.

II. Comparative Analysis of Conventional SOC Reset Algorithms

A. Principle of the Enhanced OCV Reset Algorithm

The conventional open circuit voltage (OCV) reset method has the advantage of high accuracy. However, it has the disadvantage in that it requires a long rest time. An enhanced OCV reset method is proposed in order to overcome this disadvantage [16]. In the rest-time curve, as shown in Figs. 1(a) and 1(b), there are two parts of short term effect and long term effect. The short term effect of the first part is a precipitous voltage drop of the battery, and the long term effect of the second part is a gradual voltage change which is slowly stabilized. At this time, the battery terminal voltage after the end of the short term effect is similar to the OCV in a short time. In the case of a reset using this terminal voltage, the enhanced OCV reset method has some error. However, the enhanced OCV reset algorithm has a high accuracy in the total range through frequent reset.

The reset condition of the enhanced OCV method is similar to urban driving situations, which have many stop events, in the enhanced OCV reset algorithm of Table I. Therefore, the enhanced OCV reset method has an advantage in terms of the UDDS profile since the current during rest time does not flow through the battery and the enhanced OCV reset method can operate. However, it does not operate in the various profiles of constant speed driving such as highway driving.

B. Principle of the DCIR Iterative Calculation Algorithm

As shown in Fig. 1(c), the SOC estimation algorithm by using the direct current internal resistance (DCIR) is conducted by averaging the DCIR, the terminal voltage, and the current of battery. The DCIR iterative calculation

algorithm is represented in the terminal voltage that is expressed by the sum of the OCV and the products of the DCIR and the battery current [17]. This algorithm is estimated through iterative calculations of the DCIR and OCV. It is possible to estimate an accurate value of the DCIR during the DCIR calculation process by including the direct current and terminal voltage in the constant current region. Therefore, the reset algorithm using the DCIR is able to reduce the SOC error because the algorithm conducts the reset operation in the constant current region [17]. However, the SOC accuracy, which is estimated through the DCIR algorithm, is low when the direct current is not flowing. In addition, the DCIR algorithm has a disadvantage in terms of not being able to operate in the rest regions.

The reset condition of the DCIR iterative calculation reset method is similar to the HWFET profile. This profile has many static current regions by constant speed of EVs on the highway. Therefore, the DCIR iterative calculation reset method has an advantage since it is possible to frequently reset the reference SOC through the DCIR reset. However, the DCIR iterative calculation reset method does not operate in the UDDS profile because of the rest-time region and the dynamic current of the battery. The reset conditions for these algorithms in the rest and static current regions are summarized in Table I.

TABLE I
RESETTABLE REGIONS OF VARIOUS ALGORITHMS

SOC estimation algorithm	Reset region	
	Rest region	Static current region
Coulomb counting method	Disable	Disable
Enhanced OCV reset	Enable	Disable
DCIR reset	Disable	Enable
Proposed algorithm	Enable	Enable

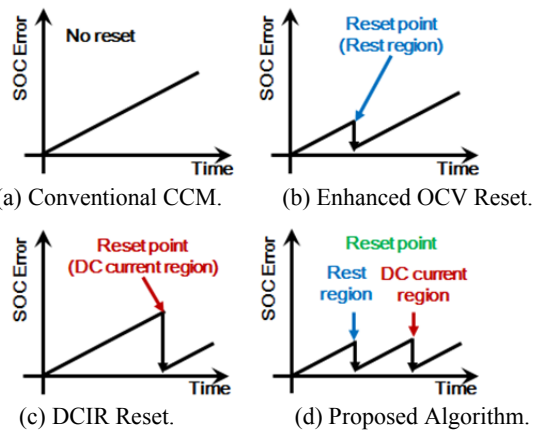

(a) Conventional CCM. (b) Enhanced OCV Reset.

(c) DCIR Reset. (d) Proposed Algorithm.

Fig. 2. SOC reset region and frequency of various algorithms.

III. PRINCIPLE OF THE PROPOSED ALGORITHM

A. *Possibility of Mixing the Two Algorithms*

As shown in Figs. 2(a) to 2(c), the accumulated SOC error is represented according to the reset region of each SOC estimation method. First, in the case of the CCM, the accumulated SOC error continuously increases because of no specific reset method, as shown in Fig. 2(a). As discussed previously, the two reset methods, i.e., the enhanced OCV reset and the DCIR reset have a reset point in a specific region, as shown in Figs. 2(b) and 2(c), respectively. The reset point of the enhanced OCV reset method is in the region where the battery current does not flow such as in urban driving patterns. Moreover, the reset point of the DCIR iterative calculation reset method is in the region where the battery current constantly flows such as in highway-driving patterns. Therefore, the two-reset methods have completely different characteristics with respect to the reset region. Thus, the principles of operation for the two-reset methods are independent.

It is possible to mix the two independent reset methods and the result is shown in Fig. 2(d). The profile of the reset point, as shown in Fig. 2(d), is a composition of the urban driving pattern in the front part and the highway driving pattern in the back part. Using the enhanced OCV reset method and the DCIR iterative calculation reset method for resetting in this profile, it is possible to reset only once. However, the proposed algorithm, which is a mix of the two-reset methods, is able to the reset the SOC twice.

B. *Advantage of a mixed algorithm*

According to the composition of the profile, each reset method has different magnitude of the SOC error. In the case of specific profiles such as the UDDS and HWFET, both the enhanced OCV reset method and the DCIR iterative calculation reset method result in large SOC errors. For example, in the case of the enhanced OCV reset method, the profile in the regions of waiting for a traffic signal occurs frequently and has many SOC reset points. However, if the profile has a few regions of waiting for a traffic signal such as the HWFET, the enhanced OCV reset does not occur. Therefore, the accumulated SOC error of the enhanced OCV reset method is equal to the conventional CCM. In contrast to the enhanced OCV reset method, the DCIR iterative calculation reset method shows opposite results in the two profiles. Thus, the proposed reset algorithm is able to obtain a smaller SOC error when compared to the conventional reset methods without specific profiles from mixture of two independent reset algorithms.

IV. VARIOUS DRIVING PATTERNS OF EVS

As mentioned in the introduction, algorithm accuracy depends on the driving pattern. In order to evaluate the driving patterns of various EVs, the proposed algorithm is compared with the conventional reset methods through a

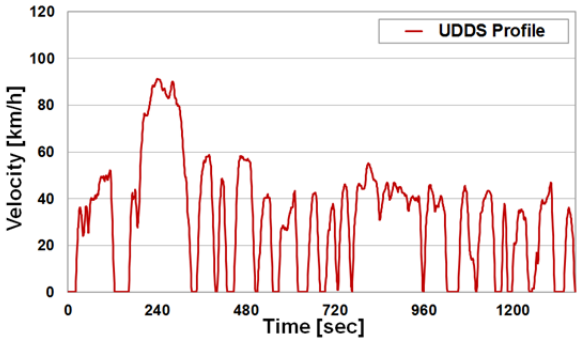

(a) UDDS velocity profile.

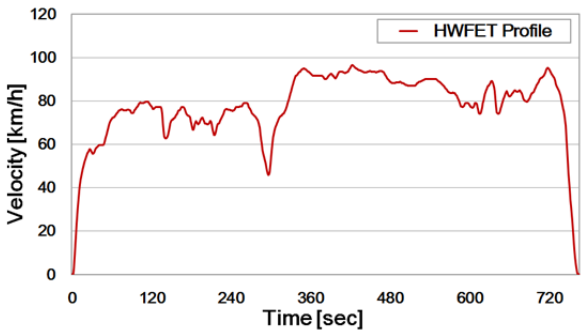

(b) HWFET velocity profile.

Fig. 3. UDDS and HWFET velocity profiles of the USEPA.

combination of conventional profiles. In general, the United States environmental protection agency (USEPA) provides a profile that is used to evaluate the fuel efficiency of EVs. The USEPA provides the UDDS profile, which imitates the urban dynamic driving pattern, and the HWFET profile, which imitates the static driving patterns on the highway. Thus, four profiles are evaluated to represent the real driving patterns of EVs.

Each individual profile of the UDDS and HWFET consumes 80% of the SOC in the same battery. However, the four driving patterns have different ratios of the UDDS and HWFET. A-profile has a SOC consumption of 8% of the UDDS profile and 72% of the HWFET profile. The change from A-profile to D-profile is that the ratio of the UDDS profile is increased, while the HWFET ratio is decreased. The performance of the algorithms is evaluated for a combination of these four profiles.

A. Conversion from Velocity Profile to the Current Profile

Both the UDDS and HWFET profiles, which are provided by USEPA, are applied to the enhanced OCV reset and DCIR reset methods. As mentioned earlier, the UDDS profile, which imitates urban driving patterns, includes many short waiting times at traffic signals. Considering the waiting time at traffic signals, the UDDS profile adds about 160 seconds of waiting time after the end of the UDDS profile in order to equal the total time of the validation profile. Fig. 3 shows the velocity profiles of the UDDS and HWFET as provided by USEPA. The current profile of a real battery is decided by the

TABLE II
AVANTE HYBRID SPECIFICATIONS [18]

Detailed items	Value [Unit]
Weight of vehicle (w)	12710.6 [N]
Equivalent weight of rotation (w')	674.73 [N]
Air resistance coefficient (u_a)	0.012 [kg·sec^2/m^4]
Rolling resistance coefficient (u_r)	0.01
Tire diameter (R_{dyn})	0.38 [m]
Height (h)	1.49 [m]
Full width (b)	1.775 [m]
Frontal projected area (A)	2.64475 [m^2]
Efficiency of motor and inverter (η)	80 [%]

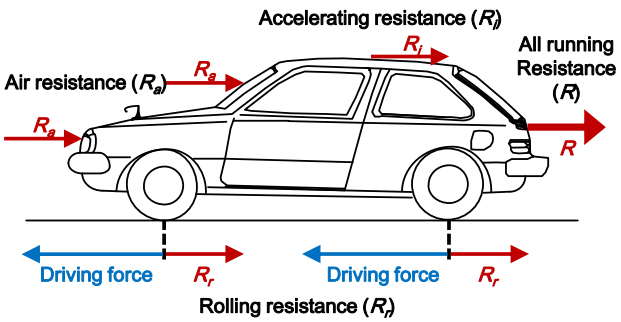

Fig. 4. Running resistance of the general vehicle [18].

specifications of the EV hardware. Hence, the profile has to be recreated to consider the system specifications.

In this paper, the current profile is determined based on the velocity profile by using the specifications of the AVANTE HYBRID and the other parameters, as shown in Table II of the reference. The 80% efficiency (η) of the 80-kW three phase inverter and interior permanent magnet synchronous motor of the AVANTE HYBRID is considered to be a very low and bad condition for EVs. As shown in Fig. 4, for driving a vehicle, the running resistance (R) should be as much as the sum of three resistances, which are the rolling resistance (R_r), the air resistance (R_a), and the acceleration resistance (R_i), as in the following equations [18] :

$$R_r = \mu_r \cdot w \tag{1}$$

where u_r is rolling resistance coefficient, and w is weight of the vehicle,

$$R_a = \mu_a \cdot A \cdot v^2 \tag{2}$$

where u_a is the air resistance coefficient, A is the frontal projected area, and v is the velocity of the vehicle,

$$R_i = \frac{w + w'}{g} \cdot a \tag{3}$$

where w' is the equivalent weight of rotation, a is the acceleration of the vehicle, and g is the gravitational acceleration,

$$R = R_r + R_a + R_i \ . \tag{4}$$

The interaction formula between the power of the mechanical

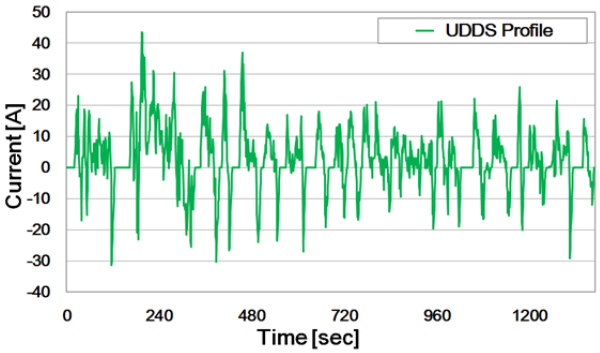

(a) UDDS current profile.

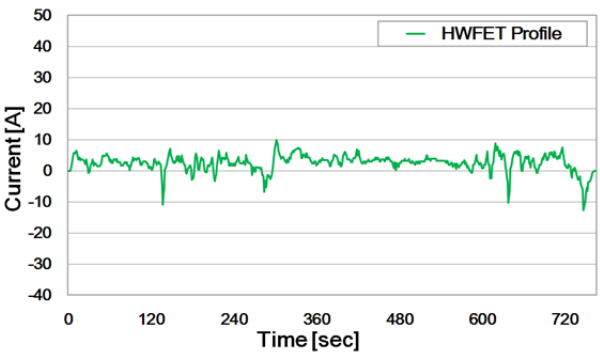

(b) HWFET current profile.

Fig. 5. Current profiles converted from velocity profiles.

system (P_m) and that of the electrical system (P_e) is expressed by:

$$\eta = \frac{P_m}{P_e} = \frac{F \cdot v}{V \cdot I} \tag{5}$$

where η is conversion efficiency from the mechanical system to the electrical system. Finally, the current profile can be derived from the velocity profile of the vehicle, as indicated by:

$$I = \frac{Fv}{\eta V}. \tag{6}$$

The current profiles are illustrated with the UDDS and HWFET as shown Figs. 5(a) and 5(b), respectively. In the current profile of the UDDS, there is the deceleration range, as shown in Fig. 5(a). It is generated from regenerative breaking, in which the battery is charged by negative current. In the current profile of the HWFET, the largest deceleration range exists at the last region of the profile, as shown in Fig. 5(b).

B. Combination of each of the Reference Profile

The combination of each current profile shown in Fig. 5 is used to create composite profiles A, B, C, and D that have different ratios of dynamic and static properties. Fig. 6(a) shows a profile that includes a lot of highway driving. This profile includes a dynamic current profile that consumes 8% of the SOC and a static current profile that consumes 72% of the SOC. It implies that the A profile discharges from a 100% SOC battery to a 20% SOC battery. A waiting time of 160 seconds for a traffic signal is inserted after the dynamic profile of the UDDS. The enhanced OCV reset is applied and the SOC is reset after the UDDS profile.

In order to apply the equal integrating error of the CCM to the A, B, C, and D profiles, each profile should have the same consumption of time and SOC. Since the experimental conditions cannot exceed the limits of the test equipment, the current scale of the UDDS profile is multiplied by a factor of 0.437, and the current scale of the HWFET profile is multiplied by a factor of 0.123. A single cycle in the UDDS consumes 4% of the SOC and has a duration of about 26 minutes, while a cycle of the HWFET consumes 2% of the SOC and has a duration of about 13 minutes. The ratio of the dynamic and static SOC consumption for profile B, which represents the mid-level driving pattern, is 32% and 48%, respectively; for profile C, which is also a mid-level driving pattern, the SOC consumption ratio is 48% dynamic and 32% static; and for profile D, which is closest to the highway driving pattern, the ratio is 72% dynamic and 8% static SOC consumption, as shown in Fig. 6.

V. THEORETICAL CONSIDERATIONS FOR MIXING

A. Effects of the Weighted Current Value I_{DC}

In order to improve the performance of the enhanced OCV reset method and the DCIR reset method, the second-order RC ladder model is mathematically analyzed to estimate the SOC of a battery as shown Fig. 7 [19]-[20]. If the voltage of the RC network inside the battery is estimated exactly, the accuracy of the SOC estimation can be improved. Therefore, a mathematical analysis of the internal impedance inside the battery is important.

$$\begin{aligned} v_T(t) &= OCV(v_{C\_SOC}(i(t))) + R_S \cdot i_T(t) \\ &+ (1-e^{-\frac{t}{R_1C_1}}) \cdot R_1 \cdot i_T(t) + (1-e^{-\frac{t}{R_2C_2}}) \cdot R_2 \cdot i_T(t) \\ &+ V_1(t_0) \cdot e^{-\frac{t}{R_1C_1}} + V_2(t_0) \cdot e^{-\frac{t}{R_2C_2}} \end{aligned} \tag{7}$$

$$V_1(t_0) = \frac{1}{C_1}\int_{-\infty}^{t_0} i_{C_1}\,dt\ ,\ V_2(t_0) = \frac{1}{C_2}\int_{-\infty}^{t_0} i_{C_2}\,dt \tag{8}$$

The second-RC ladder model of the battery is analyzed for the characteristic of a step response for the current of certain magnitude as shown in the left figure of Fig. 8(b). The terminal voltage, which is deduced as a result of the Laplace transform, is given by (7). The terminal voltage is the sum of six terms. The first term is the result of the OCV change that is influenced by the current flow of the battery. The second term is a part of a series voltage drop in the series resistance R_s. The third and fourth terms are parts of an exponential variation from the RC network. The fifth and sixth terms are parts of the initial voltage applied to the RC network inside the battery. The initial voltage $V_1(t_0)$ and $V_2(t_0)$ of the RC network can be calculated by the capacitance (C_1 and C_2) and the current of the

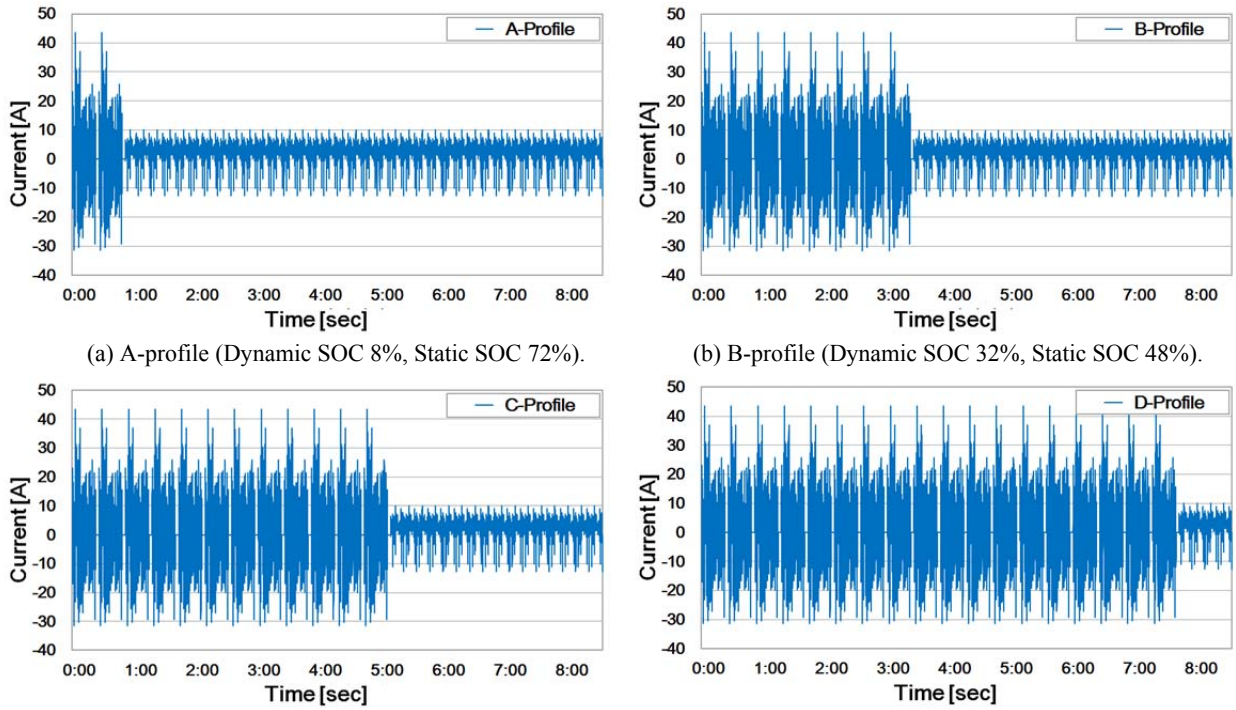

(a) A-profile (Dynamic SOC 8%, Static SOC 72%).

(b) B-profile (Dynamic SOC 32%, Static SOC 48%).

(c) C-profile (Dynamic SOC 48%, Static SOC 32%).

(d) D-profile (Dynamic SOC 72%, Static SOC 8%).

Fig. 6. Four driving profiles generated by various ratios of the UDDS and HWFET profiles.

capacitance ($i_{C1}(t)$ and $i_{C2}(t)$) in (8). Therefore, the initial voltage $V_1(t_0)$ and $V_2(t_0)$ of the RC network are complicated to calculate [21].

After the capacitance of the RC Ladder is fully charged (saturation), the internal voltage of the RC-ladder can be simply calculated by multiplying the battery terminal current and internal resistance [17]. In order to simplify the actual dynamic situation such as 3, this is the main concern when the RC-ladder is fully charged (or saturated). Therefore, the average time constant (T_A) of the two time constants (T_1 and T_2) is useful for the detection of the RC-ladder saturation. This is because the T_A can represent both of the effects of the battery dynamics: short term (T_1) effect and long term (T_2) effect.

$$V_1(t_0) = (1-e^{-\frac{t}{R_1C_1}})\cdot R_1\cdot i(t),\quad \mathrm{T}_1 = R_1C_1$$
$$V_2(t_0) = (1-e^{-\frac{t}{R_2C_2}})\cdot R_2\cdot i(t),\quad \mathrm{T}_2 = R_2C_2 \tag{9}$$

$$Ratio_{1T_A} = \frac{\int_0^{1T_A} e^{-t}dt}{Area}\times 100\ [\%]$$
$$Ratio_{2T_A} = \frac{\int_{1T_A}^{2T_A} e^{-t}dt}{Area}\times 100\ [\%],\quad Area = \int_0^{3T_A} e^{-t}dt \tag{10}$$
$$Ratio_{3T_A} = \frac{\int_{2T_A}^{3T_A} e^{-t}dt}{Area}\times 100\ [\%]$$

T_1 and T_2 are dependent on the R and C parameters resulting from the voltage curve fitting with T_1 being shorter than T_2. The LiPB, which is used in this experiment, has T_1 and T_2 values of 55 seconds and 870 seconds, respectively in (9). Therefore, the value of T_A is 463 seconds and value of the 3τ (95.02%) is used in the area factor as shown in Fig. 8 (b). In addition, by using this factor, the representative current (I_{DC}), which is matched with the constant battery current of the step response condition, can be deduced by (10) despite its actual dynamic current profile. This can facilitate the RC ladder voltage calculation. Therefore, T_A and I_{DC} are helpful for the calculation of the battery component voltage. As a result, they can make the each SOC reset algorithm more accurate.

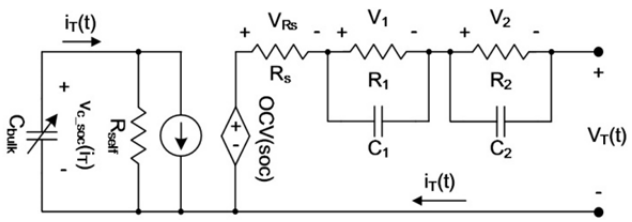

Fig. 7. Second-order RC ladder model of LiPB [19], [20].

The value of the average current that is used in the conventional reset method cannot accurately represent the voltage characteristic of the battery, as shown in Fig. 8(a). Thus, according to Fig. 8 (b), the green line dynamic current profile is multiplied by an area factor calculated from (10) when the profile is applied to the battery. The calculated I_{DC}, shown as a red line in Fig. 8 (b), is applied to the two methods. In the enhanced OCV reset method, I_{DC} is the index of the static current in the battery, and it makes voltage estimation possible during the expected rest time. The conventional enhanced OCV reset method uses the weighted current value I_{DC} during 18

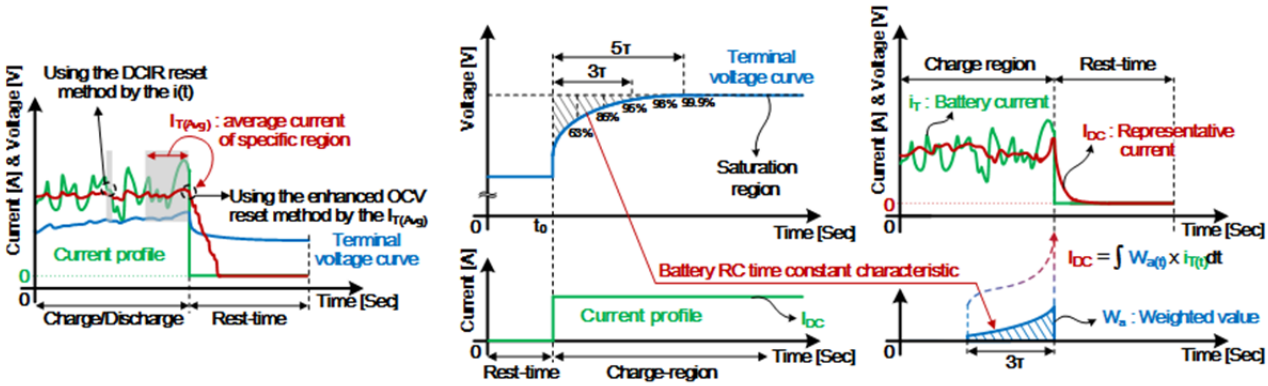

(a) Principle of the two conventional reset algorithms. (b) Calculation of representative current for the proposed algorithm.

Fig. 8. Reset method for increasing the accuracy of conventional methods and the proposed algorithm.

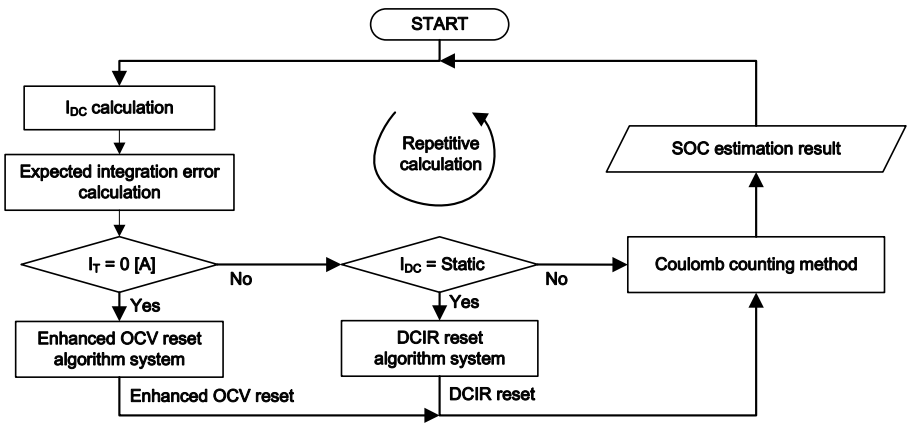

Fig. 9. Flowchart of the proposed algorithm.

minutes of the average charge and discharge rate (C-rate). In this case, the estimation does not include an increase in the voltages V_1 and V_2 during full charging of the capacitance with the second-order RC ladder model. This results in an incorrect current estimation. Therefore, the area factor reflects the current influence before the rest time. The calculated I_{DC} is also applied to the DCIR reset method. The difference between these two methods is that in the DCIR reset method, the method begins only when the instantaneous current achieves an error lower than 5% with respect to the calculated current value after 3τ. If not, the conventional CCM begins.

Applying the weighted current value I_{DC} to each method gives an improvement over the conventional method, and the SOC estimation accuracy is increased. In this paper, a flow chart of the proposed algorithm is presented as shown in Fig. 9. The weighted current value and expected error of the CCM are calculated and separated from the OCV reset method by the terminal current value. After that, the algorithm operates as the CCM and SOC reset occurs when the condition of each method is satisfied.

VI. Simulation Results

A. Simulation Platform and Evaluation Method

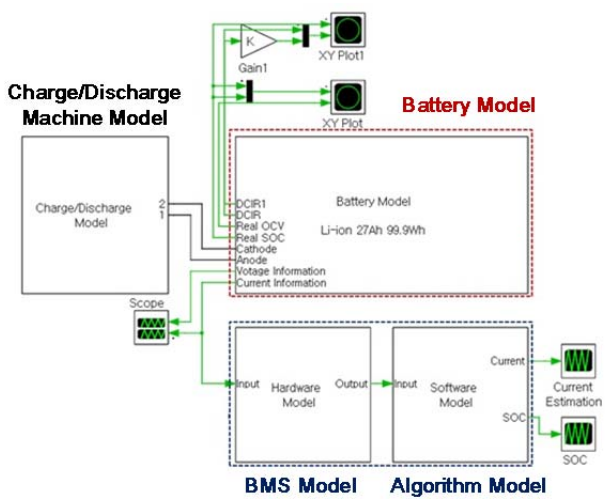

Fig. 10. PLECS simulation platform.

The Simulation platform is configured using PLECS, as shown in Fig. 10. The test profile shown in Fig. 11(a) is given as the input to the PLECS. The simulation is configured by entering the error value, which is obtained through experiments and a reference SOC. The conventional CCM, the two reset methods, and the proposed reset algorithm, which is presented in this paper, are configured in the software block and the

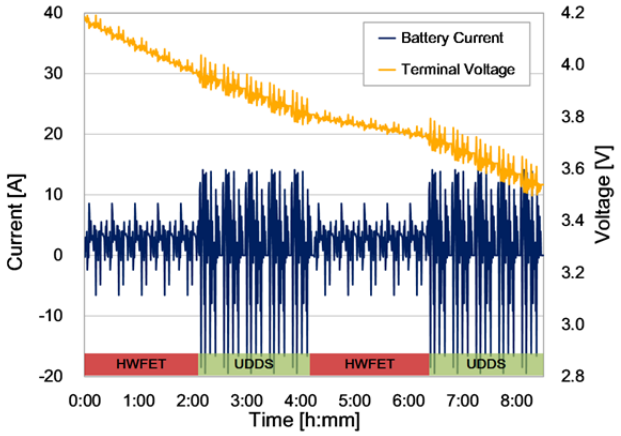

(a) Battery current and voltage of the test profile.

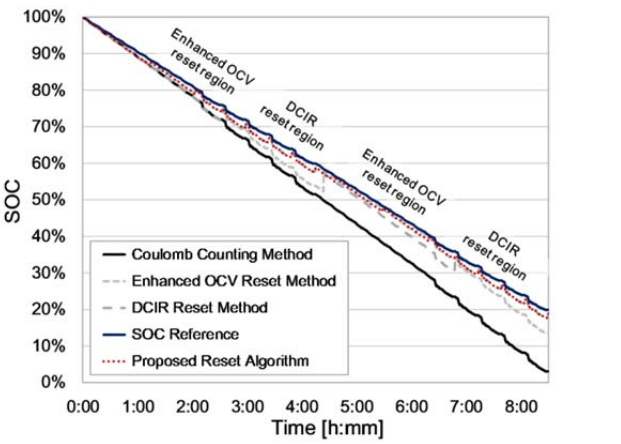

(b) Simulation result of estimated SOC for the test profile.

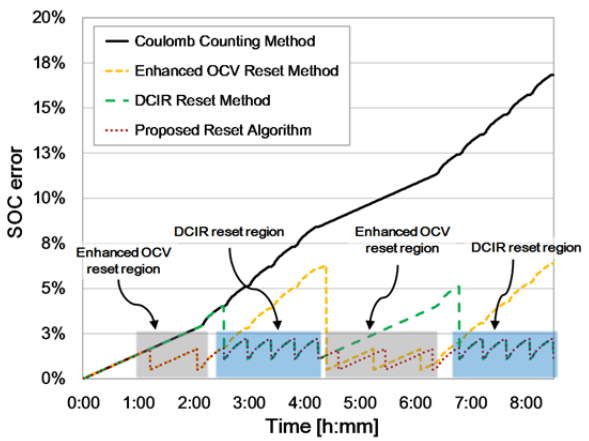

(c) SOC reset region of test profile.

Fig. 11. Simulation results of the test profile.

simulations are performed through the PLECS program.

The test profiles are simulated by four methods (coulomb counting method, enhanced OCV reset method, DCIR reset method, and the proposed algorithm). In order to verify that the proposed algorithm effectively removes the accumulated error of the CCM, the results of the proposed algorithm are compared with the those of the SOC estimations for the CCM and the two reset algorithms (the enhanced OCV reset

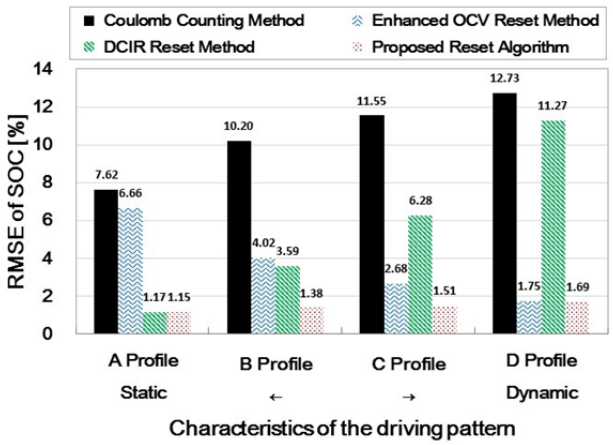

Fig. 12. Simulation results of SOC RMSE for each profile.

algorithm and the DCIR iterative calculation reset algorithm). The root mean square error (RMSE) of the estimated SOC result is used to verify the SOC error during battery usage. As shown in Fig. 11(b) and 11(c), the proposed algorithm has frequent reset events. As a result, its estimated SOC is closer to the reference SOC than the other methods. The total period of the test profile is 8 hours and 30 minutes and the RMSE of the estimated SOC during this period is calculated by (11). The RMSEs of the SOC for the CCM and the proposed algorithm are 6.59% and 1.48%, respectively, as shown in Fig 11. The RMSE of the SOC for the test profile using the simulation when compared to the CCM is reduced by 5.11%. As a result, it is confirmed that the proposed algorithm is more accurate than each of the reset methods.

$$RMSE_{SOC}[\%] = \sqrt{\frac{\sum_{i=1}^{N}(SOC_{ref,i} - SOC_{method,i})^2}{N}} \quad (11)$$

Using the same method, simulations were conducted for the four types of profiles mentioned in the previous paragraph. As a result, the average SOC RMSE of the proposed method is 1.44%, which is reduced by 9.09% when compared to the 10.52% of the CCM results as shown in Fig. 12. In addition, the SOC RMSEs of the four profiles are always under 1.69% in the proposed method.

VII. Experimental Results

In this paper, the experimental set is a BMS test bed as shown in Fig. 13(a). It consists of a microcontroller (TI's DSP TMS320F28335), a current sensor (LEM's HAS 500-P), and a circuit breaker. A 4-channel single cell charging and discharging machine with a rating up to 50-A is used for charging and discharging the battery. The charging and discharging machine is shown in Fig. 13(b). Additionally, an emulator (RealSYS's RealDSP-UT) is used to connect to the computer for communication. In addition, the UDDS and HWFET profiles, which are provided by the USEPA, are

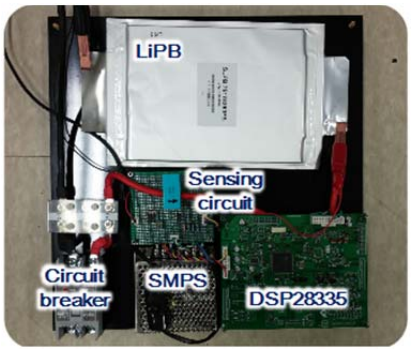

(a) BMS test bed.

(b) Charging and discharging machine.

Fig. 13. Configuration of BMS hardware.

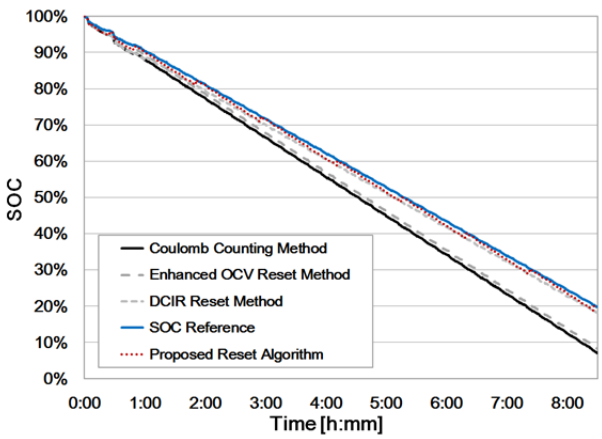

(a) Experimental results of the A-profile.

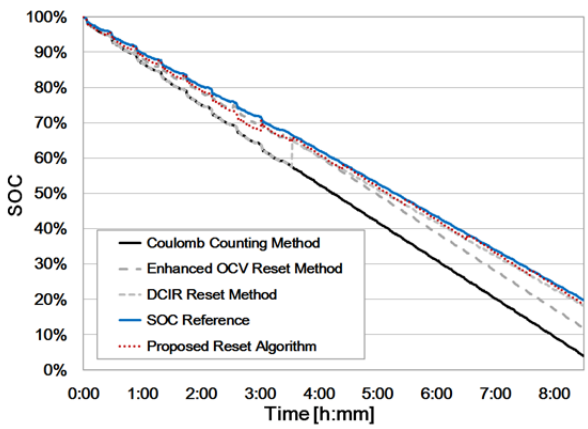

(b) Experimental results of the B-profile.

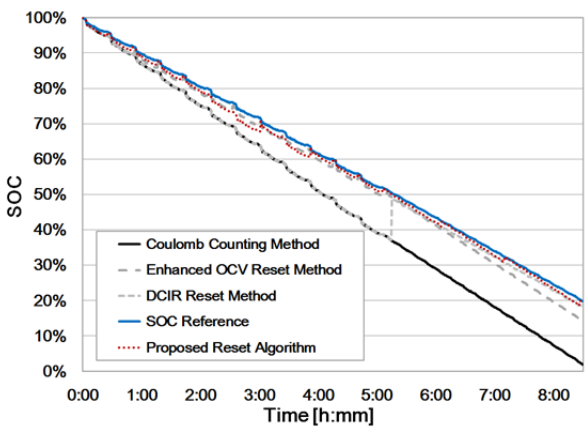

(c) Experimental results of the C-profile.

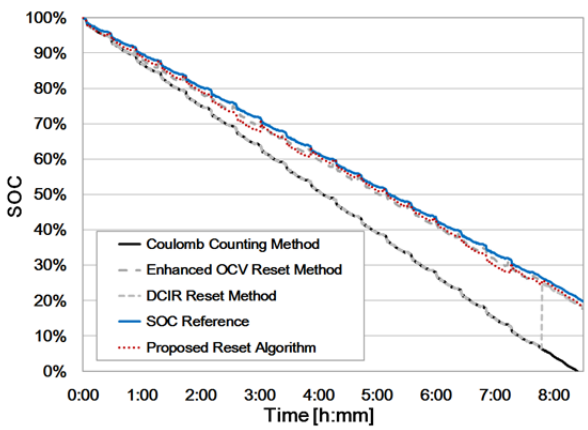

(d) Experimental results of the D-profile.

Fig. 14. Experimental results of the estimated SOC for each profile.

applied to the battery in the experiment using the exclusive program of charging and discharging.

The experiments are performed using a Kokam 27-Ah LiPB and a charging and discharging device of 50-A rating at 25 ºC. The experimental results show an improved value of the weighted current value I_{DC} with respect to the target current for the A, B, C, and D profiles as shown in Fig. 14. In the experiment, the reset points of the proposed reset algorithm can be improperly generated due to inaccuracy in the model parameter and the sensing noise of the battery current and/or voltage. Therefore, the accuracy of the experimental results can be lower than that of the simulation results which do not consider sensing noise and model inaccuracy. The SOC RMSE of the proposed algorithm is lower than that of the conventional CCM, the enhanced OCV reset method, and the DCIR reset method, regardless of the driving pattern type. As a result, the average SOC RMSE of the proposed method is 1.36%, which is reduced by 9.16% compared to the 10.52% of the CCM results as shown in Fig. 15. In addition, the SOC RMSEs of the four profiles are always under 1.72% in the

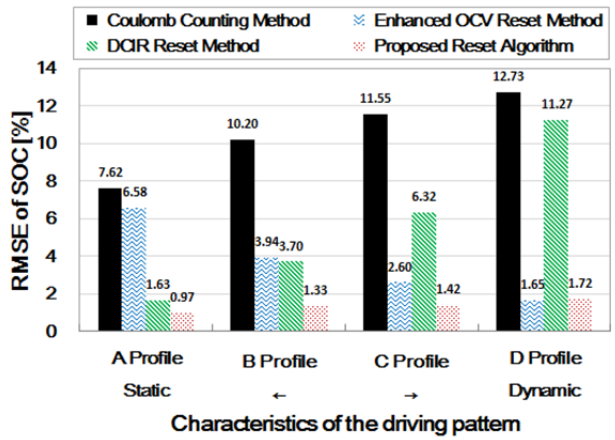

Fig. 15. Experimental results of SOC RMSE for each profile.

proposed method, which is significantly accurate compared to the existing method results (CCM: 12.73%, DCIR: 11.27%, OCV: 6.58%). Thus, it is confirmed that the proposed mixed algorithm is more accurate than the reset methods.

VIII. Conclusion

In this paper, an SOC estimation algorithm is proposed to reduce the accumulated SOC error of the CCM. The proposed algorithm mixes the enhanced OCV reset method and the DCIR reset method through an increase of the reset frequency in the driving pattern. In addition, the two conventional methods are verified by the converted and applied weighted current value I_{DC}. It can be seen from the experimental results that the SOC RMSE of the A, B, C, and D profiles are reduced by 6.65%, 8.86%, 10.13%, and 11.01%, respectively, in comparison to the CCM. As a result, the average RMSE of the SOC is reduced by 9.16%. Although the proposed SOC estimation algorithm is tested in a long driving pattern with a duration of 8 hours and 30 minutes, the average RMSE of the four profiles is under 1.72% which is always lower than the conventional methods. Therefore, the proposed algorithm has a high accuracy for the various driving patterns of drivers which further increases the maintenance and management performance of the battery management system.

Acknowledgment

This work was supported by the Industrial Strategic Technology Development Program (No.10053710) funded by the Ministry of Trade, Industry & Energy (MI, Korea).

References

[1] K. W. E. Cheong, B. P. Divakar, H. J. Wu, K. D. K. Ding, and H. F. Ho, "Battery-management system (BMS) and SOC development for electrical vehicles," *IEEE Trans. Veh. Technol.,* Vol. 60, No. 1, pp. 76-88, Jan. 2011.

[2] D. J. Lim, J. G. Kim, J. H. Ahn, D. H. Kim, and B. K. Lee, "A mixed SOC estimation algorithm using enhanced OCV reset and the DCIR iterative calculation reset," *IEEE Conference on ECCE Asia (ICPE-ECCE Asia),* pp. 1155-1160, 2015.

[3] A. Manenti, A. Abba, A. Merati, S. M. Savaresi, and A. Geraci, "A new BMS architecture based on cell redundancy," *IEEE Trans. Ind. Electron.,* Vol. 58, No. 9, pp. 4314-4322, Sep. 2011.

[4] J. Xu, C. C. Mi, B. Cao, J. Deng, Z. Chen, and S. Li, "The state of charge estimation of lithium-ion batteries based on a proportional-integral observer," *IEEE Trans. Veh. Technol.,* Vol. 63, No. 4, pp. 1614-1621, May 2014.

[5] S. Piller, M. Perrin, and A. Jossen, "Methods for state-of-charge determination and their applications," *Journal of Power Sources,* Vol. 96, pp. 113-120, Jan. 2001.

[6] K. S. Ng, C. S. Moo, Y. P. Chen, and Y. C. Hsieh, "Enhanced coulomb counting method for estimating state-of-charge and state-of-health of lithium-ion batteries," *Journal of Applied Energy,* Vol. 86, No. 9, pp. 1506-1511, Sep. 2009.

[7] G. L. Plett, "Extended Kalman filtering for battery management systems of LiPB-based HEV battery packs Part 1. Background," *Journal of Power Sources,* Vol. 134, No. 2, pp. 252-261, Aug. 2004.

[8] D. Xu, X. Huo, X. Bao, C. Yang, H. Chen, and B, Cao, "Improved EKF for SOC of the storage battery," *IEEE International Conference on Mechatronics and Automation,* pp. 1497-1501, 2013.

[9] S. Sepasi, R. Ghorbani, and B. Y. Liaw, "A novel on-board state-of-charge estimation method for aged Li-ion batteries based on model adaptive extended Kalman filter," *Journal of Power Sources,* Vol. 245, pp. 337-344, Jan. 2014.

[10] R. Xiong, X. Gong, C. C. Mi, and F. Sum, "A robust state-of-charge estimator for multiple types of lithium-ion batteries using adaptive extended Kalman filter," *Journal of Power Sources,* Vol. 243, pp. 805-816, Dec. 2013.

[11] C. Mohammad and F. Mohammad, "State-of-charge estimation for lithium-ion batteries using neural networks and EKF," *IEEE Transaction on Industrial Electronics,* Vol. 57, No. 12, pp. 4178-4187, Dec. 2010.

[12] Z. Chen and Y. Fu, "State of charge estimation of lithium-ion batteries in electric drive vehicles using extended Kalman filtering," *IEEE Trans. Veh. Technol.,* Vol. 62, No. 3, pp. 1020-1030, Mar. 2013.

[13] X. Lu, K. L. V. Iyer, K. Mukherjee, and N. C. Kar, "A dual purpose triangular neural network based module for monitoring and protection in bi-directional off-board level-3 charging of EV/PHEV," *IEEE Trans. Smart Grid,* Vol. 3, pp. 1670-1678, Aug. 2012.

[14] I. H. Li, W. Y. Wang, S. F. Su, and Y. S. Lee, "A merged fuzzy neural network and its applications in battery state-of-charge estimation," *IEEE Trans. Energy Convers.,* Vol. 22, No. 3, pp. 697-708, Sep. 2007.

[15] T. Weigert, Q. Tian, and K. Lian, "State-of-charge prediction of batteries and battery–supercapacitor hybrids using artificial neural networks," *Journal of Power Sources,* Vol. 196, pp. 4061-4066, Apr. 2011.

[16] Y. M. Jeong, Y. K. Cho, J. H. Ahn, S. H. Ryu, and B. K. Lee, "Enhanced coulomb counting method with adaptive SOC reset time for estimating OCV," *Energy Conversion Congress and Exposition,* pp. 4313-4318, 2014.

[17] Y. K. Cho, Y. M. Jeong, J. H. Ahn, S. H. Ryu, and B. K. Lee, "A new SOC estimation algorithm without integrated error using DCIR repetitive calculation," *International Conference on Electrical Machines and Systems,* pp. 865-870, 2014.
[18] S. R. Lee, B. O. Lim, J. R. Ha, and W. B. Kim, *Automotive Engineering*, Bosungkak, Chap. 4, 1996.
[19] H. Rahimi-Eichi, F. Baronti, and M. Y. Chow, "Online adaptive parameter identification and state-of-charge coestimation for lithium-polymer battery cells," *IEEE Trans. Ind. Electron.,* Vol. 61, No. 4, pp. 2053-2061, Apr. 2014.
[20] Z. Miao, L. Xu, V. R. Disfani, and L. Fan, "An SOC-based battery management system for microgrids," *IEEE Trans. Smart Grid,* Vol. 5, No. 2, pp. 966-973, Mar. 2014.
[21] W. Wang, H. S.-H. Chung, and J. Zhang, "Near-real-time parameter estimation of an electrical battery model with multiple time constants and SOC-dependent capacitance," *IEEE Trans. Power Electron.*, Vol. 29, No. 11, pp. 5905-5920, Nov. 2014.

Dong-Jin Lim received his B.S. degree in Control Instrumentation Engineering from Hanbat National University, Daejeon, Korea, in 2013. Since 2014, he has been working towards his M.S. degree at Sungkyunkwan University, Suwon, Korea. His current research interests include battery management systems (BMS) and AC-DC boost PFC converters using WBG semiconductors for home appliances.

Jung-Hoon Ahn received his M.S. degree from Sungkyunkwan University, Suwon, Korea, in 2013. Since 2013, he has been working towards his Ph.D. degree at Sungkyunkwan University. His current research interests include battery management systems (BMS), DC-DC converters for PHEV/EV and advanced motor drive systems.

Dong-Hee Kim received his B.S., M.S., and Ph.D. degrees from Sungkyunkwan University, Suwon, Korea, in 2009, 2011, and 2015 respectively. Since 2015, he has been working as a postdoctoral research associate at Sungkyunkwan University. His current research interests include PCSs and DC-DC converters for renewable energy, and battery chargers for HEVs/EVs.

Byoung Kuk Lee received his B.S. and M.S. degrees from Hanyang University, Seoul, Korea, in 1994 and 1996, respectively, and his Ph.D. degree from Texas A&M University, College Station, TX, USA, in 2001, all in Electrical Engineering. From 2003 to 2005, he has been a Senior Researcher at Power Electronics Group, Korea Electrotechnology Research Institute (KERI), Changwon, Korea. From 2006, Dr. Lee joins at College of Information and Communication Engineering, Sungkyunkwan University, Suwon, Korea. His research interests include on-board charger and wireless power transfer for electric vehicles, energy storage systems, hybrid renewable energy systems, dc distribution systems for home appliances, power conditioning systems for fuel cells and photovoltaic, modeling and simulation, and power electronics. Prof. Lee is a recipient of Outstanding Scientists of the 21st Century from IBC and listed on 2008 Edition of Who's Who in America and 2009 Edition of Who's Who in the World. Prof. Lee is an Associate Editor in the IEEE Transactions on Industrial Electronics and Guest Associate Editor in the IEEE Transactions on Power Electronics. He was the Presenter for Professional Education Seminar with the topic of "On-Board Charger Technology for EVs and PHEVs" at IEEE Applied Power Electronics Conference in 2014 and was the General Chair for IEEE Vehicular Power and Propulsion Conference (VPPC) in 2012.